ISTITUTO NAZIONALE DI FISICA NUCLEARE

Sezione di Milano

INFN/TC–97/07
25 Febbraio 1997

E. Acerbi, G. Ambrosio, M. Sorbi, G. Volpini:

THERMAL AND ELECTRICAL BEHAVIOUR OF A RESISTIVE JUNCTION IN THE ATLAS TOROIDS

SIS–Pubblicazioni
dei Laboratori Nazionali di Frascati

INFN – Istituto Nazionale di Fisica Nucleare
Sezione di Milano

INFN/AE–97/07
25 Febbraio 1997

THERMAL AND ELECTRICAL BEHAVIOUR OF A RESISTIVE JUNCTION IN THE ATLAS TOROIDS

E. Acerbi, G. Ambrosio, M. Sorbi, G. Volpini
INFN – Sezione di Milano, Laboratorio LASA and Dipartimento di Fisica dell'Università di Milano, via fratelli Cervi 201, 20090 Segrate (MI), Italy

ABSTRACT

This paper presents the results of the studies carried out at LASA on the temperature distribution along the ATLAS conductor produced by the power dissipation in a resistive junction.

From this analysis a rule has been derived to determine the maximum resistance of the junction that allows to retain a large safety margin for the stability.

Furthermore the resistance of different types of junction for the ATLAS conductor has been evaluated with a 2D code in order to verify which satisfies the limit imposed by the previous analysis.

1 INTRODUCTION

In the ATLAS magnets (Barrel Toroid and Bo) several junctions in the conductor are foreseen. namely:

- a) between the two pancakes of each section of the coil;
- b) between the two sections of the coil:
- c) between two adiacent coils of the toroid.

The problem of the junction assumes a relevant aspect in the ATLAS magnet because it is cooled indirectly and the operating current is very high ($\sim 20\,kA$). In the previous superconducting magnets or solenoids the power dissipated in the junction was only of the order of $10^{-3} \div 10^{-2}\,W$ with a junction resistance of a few $10^{-9}\,\Omega$. In the ATLAS magnet the power dissipated in the junction can reach values in the range $10^{-1} \div 10^{0}\,W$.

It is important in this case to determine the upper limit in the power dissipated in the junction (in other words the maximum resistance of the junction) that maintains a large stability margin. At our knowledge this problem has not been examined in details up to now so that there are not useful guidelines or rules for the specification of the upper limit of the junction resistance.

In the next paragraphs the thermal process in the junction will be examined for the following configurations:

- a) the junction has a very short length so that the Joule power is concentrated at the center of the junction;
- b) the junction has a finite length so that the Joule power is distributed uniformly along the junction;
- c) the junction does not exchange heat with the casing or a cooled support.

The first case represents a conservative hypothesis, the second one represents the normal situation, the third one represents an anomalous situation and it has been studied in order to have an useful warning in the assembly of the junctions placed outside of the casing.

The basic hypotheses in the process analysis are:

- 1) the only relevant solutions are the steady state ones;
- 2) the maximum temperature increase $(\theta_{max} - \theta_o)$ in the conductor must be a small fraction of the temperature stability margin $(\theta_g - \theta_o)$, being θ_o the operating temperature of the magnet and θ_g the sharing temperature of the superconductor. Tipically it is reasonable to require that:

$$\theta_{max} - \theta_o \sim 0.1(\theta_g - \theta_o) \tag{1}$$

- 3) the heat is propagating along the Al matrix of the conductor and it is transferred to the casing (or to the cooled support) through a thin insulating ribbon of constant thickness and thermal conductivity.

These hypotheses are reasonable and in particular the first hypothesis can be considered valid because the power dissipated in the junction increases very slowly during the coil excitation so that at any time there is the temperature gradient that allows the transfer of the heat along the conductor and towards the casing by avoiding an instantaneous large increase of the conductor temperature (like in the case of a local thermal disturbance). This qualitative consideration is confirmed by the low time constant of the thermal diffusivity ($\tau_d \sim 1\,s$) compared with the magnet ramping time ($\Delta t \sim 4000 \div 5000\,s$).

Further minor hypotheses will be made during the analytical study of the process, in any case the choice of the model or of the parameters will be always conservative.

The study will be completed with the calculation by means of a 2D code of the resistance of the junction in the ATLAS conductor for three different configurations:

- i) the two conductors are welded along the narrow side of the pure Al matrix;
- ii) the two conductors are welded along the large side of the pure Al matrix;
- iii) the two Rutherford cables are soldered along their large side.

and the results compared with the previous ones obtained by the thermal analysis.

From this study the specifications for the junction and its assembly has been desumed.

2 THERMAL ANALYSIS

2.1 Junction of negligible length

In this case the steady state equation is given by:

$$kS\frac{d^2\theta}{dx^2} - k_{is}\frac{p}{\Delta}(\theta - \theta_o) + \delta(x)RI^2 = 0 \tag{2}$$

where:

- k is the thermal conductivity of the matrix,
- k_{is} is the thermal conductivity of the insulation against the casing (or the cooled support);
- p is the perimeter of the conductor that is in contact with the casing (or the cooled support) through the insulation;
- S is the cross section of the conductor matrix;
- Δ is the tickness of the insulation against the casing (or the cooled support);
- θ_o is the operating temperature of the casing (or the cooled support);
- R is the junction resistance;
- I is the maximum operating current;
- $\delta(x)$ is the Dirac's delta.

The first term in the equation (2) represents the heat flow along the conductor, the second term represents the heat transferred from the conductor to the casing (or the cooled support) and the third term describes an heat source localized at $x = 0$. In order to obtain conservative results the heat transferred towards the adjacent conductors has not been considered.

The solution of the equation (2) is given by:

$$\theta = \theta_o + Ae^{-|x|/\lambda} \tag{3}$$

where:

$$\lambda = (\frac{kS\Delta}{k_{is}p})^{1/2} \quad and \quad A = \theta_{max} - \theta_o = \frac{RI^2\Delta}{2k_{is}p\lambda} \tag{4}$$

being θ_{max} the highest temperature in the cable, reached at the junction ($x = 0$) and A represents the maximum temperature drop. The modulus of the argument in the equation (3) allows the description of the temperature distribution in the left and right sides of the junction. The parameter λ represents a characteristic length of the thermal process that tipically assumes values in the range $10^{-1} \div 10^{0}\, m$. It is clear that the hypothesis of a punctual release of the Joule power is valid when the junction length L fulfils the following condition:

$$L \ll \lambda \tag{5}$$

The maximum admissible resistance of the junction for a given temperature drop can be deduced from the equation (4):

$$R_{max} = 2k_{is}\frac{p}{\Delta}(\theta_{max} - \theta_o)\frac{\lambda}{I^2} \tag{6}$$

2.2 Junction of finite length

In this case the steady state is described by a system of two equations:

$$kS\frac{d^2\theta}{dx^2} + \frac{RI^2}{L} - k_{is}\frac{p}{\Delta}(\theta - \theta_o) = 0 \tag{7}$$

$$kS\frac{d^2\theta}{dx^2} - k_{is}\frac{p}{\Delta}(\theta - \theta_o) = 0 \tag{8}$$

The first equation (valid for $-L/2 \leq x \leq L/2$) describes the heat flow in the junction by considering that the Joule power is uniformly distributed along the length L of the junction. The second equation (valid for $|x| \geq L/2$) represents the heat flow outside the junction. For conservative reasons the cross section S of the junction has been assumed equal to the cross section of the conductor.

The solution of the system is:

$$\theta(x) = \theta_o + (1 - e^{-L/2\lambda}\cosh(x/\lambda))\frac{RI^2\Delta}{k_{is}pL} \qquad |x| \leq L/2 \tag{9}$$

$$\theta'(x) = \theta_o + \sinh(L/2\lambda)e^{-|x|/\lambda}\frac{RI^2\Delta}{k_{is}pL} \qquad |x| \geq L/2 \tag{10}$$

The upper limit of the junction resistance is given in this case by:

$$R_{max} = k_{is}\frac{p}{\Delta}\frac{\theta_{max} - \theta_o}{I^2}\frac{L}{1 - e^{-L/2\lambda}} \tag{11}$$

that can be deduced from eq.(9), by considering that θ_{max} is reached at $x = 0$.

2.3 Junction of finite length without heat transfer

In this case the heat produced by the Joule effect in the resistive junction is not transferred to the casing (or the cooled support) along the whole length L of the junction. The heat flow along the junction and along the rest of the conductor is described by the following system:

$$kS\frac{d^2\theta}{dx^2} + \frac{RI^2}{L} = 0 \tag{12}$$

$$kS\frac{d^2\theta}{dx^2} - k_{is}\frac{p}{\Delta}(\theta - \theta_o) = 0 \tag{13}$$

whose solution is:

$$\begin{aligned} \theta(x) &= \theta_o + \frac{RI^2}{2kS}(\lambda + L/4 - x^2/L) \qquad |x| \le L/2 \\ \theta'(x) &= \theta_o + \frac{RI^2\lambda}{2kS}e^{-(|x|-L/2)/\lambda} \qquad |x| \ge L/2 \end{aligned} \tag{14}$$

As in the previous case, the highest resistance admissible for a given maximum temperature increment, can be found from the first equation of the system (14), by keeping in mind that the highest temperature is reached at $x = 0$:

$$R_{max} = \frac{2k_{is}p(\theta_{max} - \theta_o)\lambda}{I^2\Delta(1 + L/4\lambda)} \tag{15}$$

2.4 Comparison of the results

Fig. 1 shows the typical temperature behaviour along the cable for the three examined cases.

It is clear that the most critical situation is represented by the third case (no heat exchange along the junction), for which an increase of the junction length reduces the maximum admissible value of the resistance as shown by eq. (15).

For the comparison and for the electrical analysis it is useful to define the specific resistance Φ:

$$\Phi = R \times L \tag{16}$$

which is independent on the welding length (provided that end effects can be neglected), since it is a function only of the geometry of the cross-section, and of the resistivity of the interfaces, matrix bulk and welded (or soldered) region. In the hypothesis that the interface and welding resistances are negligible the function Φ can be described by:

$$\Phi = \epsilon\rho\frac{d}{a} \tag{17}$$

being ρ the resistivity of the matrix, d the minimum distance between the two Rutherford cables, a the width of the welded (or soldered) region between the two conductors and ϵ an adimensional correcting factor that must be determined through an electrical analysis of the junction.

The resistive function Φ of the welding must fulfil the following conditions:

$$\Phi \le \Phi_{max} = 2k_{is}\frac{p}{\Delta}(\theta_{max} - \theta_o)\frac{\lambda L}{I^2} \tag{18}$$

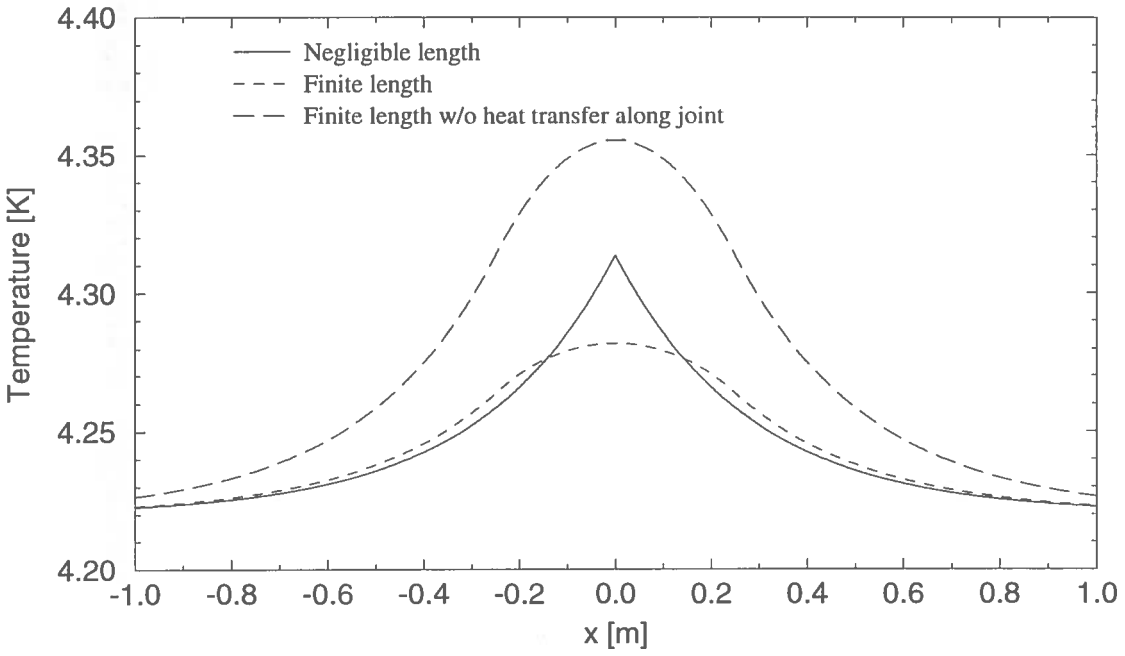

FIG. 1: An example of the temperature distribution in the junction and the conductor for the three examined cases, when $L = 0.5\,m$ and $RI^2 = 0.42\,W$.

$$\Phi \leq \Phi_{max} = k_{is}\frac{p}{\Delta}\frac{(\theta_{max} - \theta_o)}{I^2}\frac{L^2}{1 - e^{-L/2\lambda}} \tag{19}$$

$$\Phi \leq \Phi_{max} = 2k_{is}\frac{p}{\Delta}\frac{\theta_{max} - \theta_o}{I^2}\frac{L\lambda}{1 + L/4\lambda} \tag{20}$$

obtained from the relations (6), (11) and (15).

The first two equations (case a) and case b)) can be fulfilled by a suitable value of the junction length L, the third equation can be fulfilled only if the following condition (obtained by the equation (20) for $L \to \infty$) is satisfied:

$$\Phi < \Phi_\infty = 8(\theta_{max} - \theta_o)\frac{kS}{I^2} \tag{21}$$

From this analysis it is clear that the designer of the junction must verify at first if the condition (21) can be fulfilled. If yes the maximum resistance R_{max} and the minimum length L_{min} of the junction can be derived from the equation (20): in this case there is a large safety margin also if the junction has not a good thermal contact with the casing (or the cooled support). If not the designer will derive the conservative value of R_{max} and the junction length L_{min} from the equation (18): in this case he must be absolutely sure that there is a good thermal contact of the junction with the casing (or the cooled support).

3 ELECTRICAL ANALYSIS

3.1 Junction schemes

This paragraph shows a study of the power dissipation in three of the most used types of junction for magnet with indirect cooling. Their cross section is sketched in Fig. 2.

The first type of junction can be very useful during the double pancake winding (no bending of the conductor, minimum encumbrance) but it will present the highest resistance. The second and third type of junction give lower resistances but require more complicated operations during the coil winding.

The aim of the following analysis is the calculus of the Φ function and of the margin against the stringent condition (15) for each junction.

The Φ function depends on the geometry and the electrical properties of each component of the superconductor. In particular:

- the stabilizer-matrix interface;
- the matrix;
- the welded or soldered region.

Because of the geometry a numerical analysis has been performed. Since the value of the resistance of the matrix-cable interface is unknown, the study has been parametric. Being also the welding technique not jet fixed, the resistances has been calculated for two different welding depth. At the end all the results are summarized in case of the foreseen value of the matrix-cable interface resistance and of the worst welding depth.

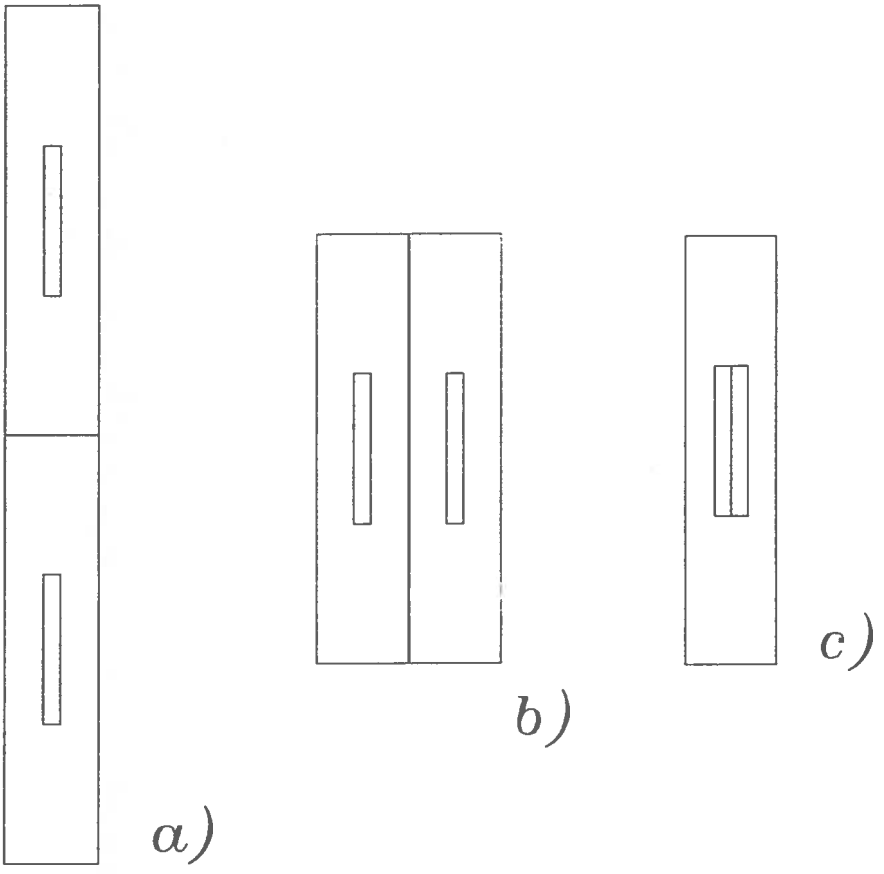

FIG. 2: Geometry of the different types of junction for an indirectly cooled magnet: a) narrow side welding b) broad side welding c) insert soldering.

3.2 Description of the models

The resistance of the first and second type of junction shown in Fig. 2 have been computed throught a 2D electrostatic analysis performed with the electromagnetic code POISSON.

The simplest model is shown in Fig. 3a. It was used to analyse the effect of the conductor geometry on the whole resistance without taking into account the resistance of the stabilizer-matrix interface. The outer rectangle of the model has the dimensions of the conductor cross section, the inner has the dimensions of the insert cross section.

The main assumptions in the model are:

- the insert surface is equipotential ($V = V_0$);
- the welded surface is equipotential ($V = 0$);
- the electric field is normal to the welded surface and tangential to the other boundaries of the conductor.

The first assumption, which neglects the internal structure of the insert, is based on the fact that the resistances between the filaments and between the strands in the insert are very low (tipically a few $10^{-12}\,\Omega\,m$). The second and third assumptions arise from the symmetry of the model.

The pattern of the electric field (E_{static}) due to this potential difference is the same of the elctric field ($E = \rho J$) generated by the current flowing from one cable to the other having the same boundary conditions (Neumann problem). The potential difference due to the current flow (ΔV) can be obtained by scaling the potential difference of the electrostatic problem ($\Delta V_{static} = 2V_0$). The scaling factor (k) is derived considering that all the current (I) must cross the welded surface being normal to the surface itself. Therefore on the welded surface (S) it is:

$$\int_S E\, dS = \int_S \rho J\, dS = \rho I \tag{22}$$

where ρ is the resistivity of the welded surface. The scaling factor is:

$$k = \frac{\int_S E_{static}\, dS}{\rho I} \tag{23}$$

and the resistance is:

$$R = \frac{2V_0}{kI} = \frac{2V_0\rho}{L \int_l E_{static}\, dl} \tag{24}$$

being l the weld line in the 2D model, and L the lenght of the weld in longitudinal direction.

Fig. 3c shows the model adopted to compute the whole resistance by considering also the contact resistance between the stabilizer and the matrix. It's the same model of the previous case with another little inner rectangle whose surface is the new equipotential surface ($V = V_0$). The region between the two inner rectangles is used to simulate the interface region. The thickness of this region is greater than what is foreseen because of meshing requirements. Three resistivities for this region were computed in order to have a contact resistance of 1, 0.1 and 0.01 $n\Omega$ on a 1 meter sample. The ratio between these resistivities and the Aluminum resistivity (RRR=500) was used to obtain the electrical permittivity of the interface for the electrostatic analysis.

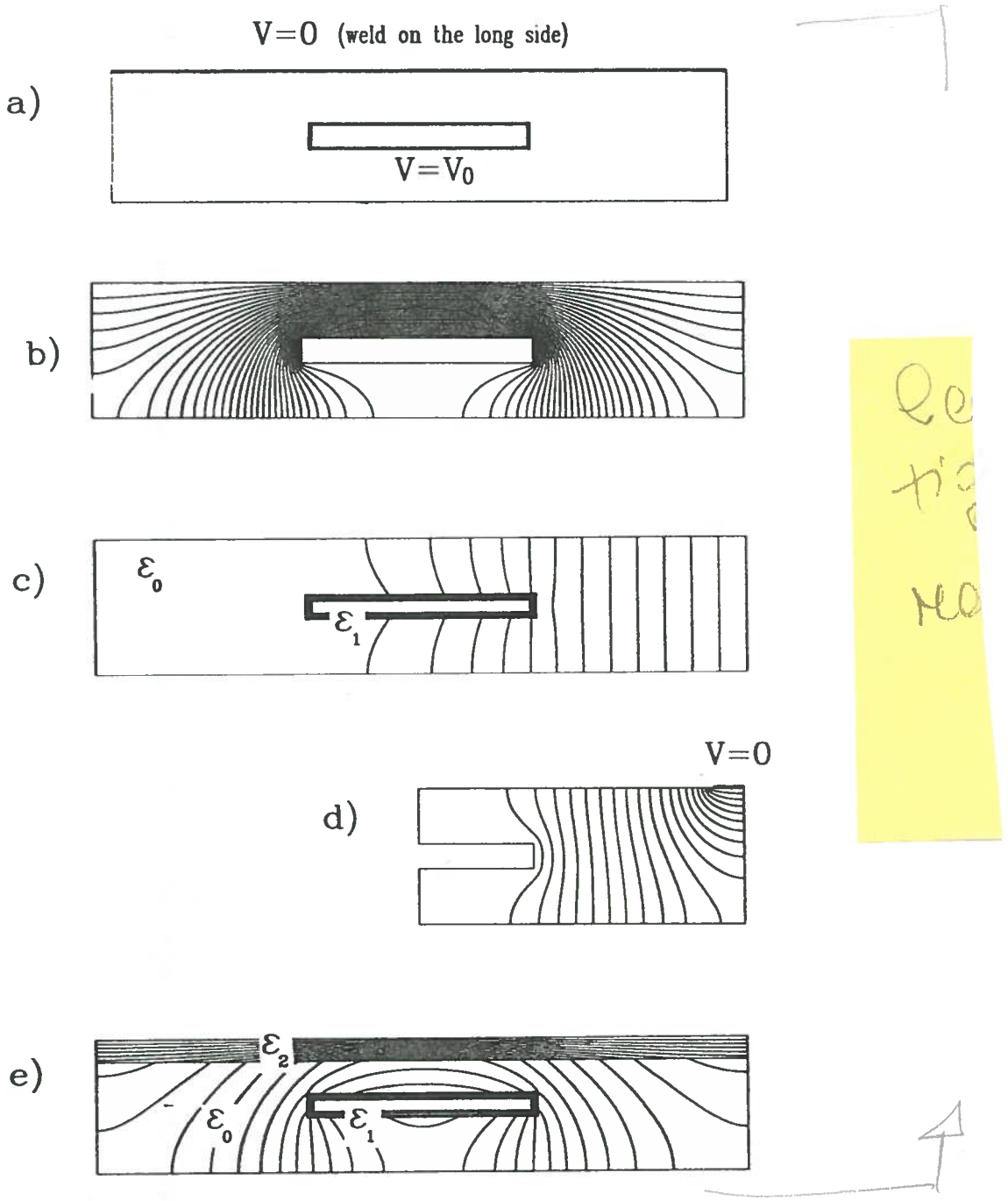

FIG. 3: Some models used and their equipotential surfaces distribution: a) geometry and equipotential surfaces imposed at some boundaries; b) welding on the broad side; c) welding on the narrow side and interface resistance: $R_{if} * L = 0.1 n\Omega\, m$; d) welding on the broad side only 3 mm deep; e) welding on the broad side with Al degradation and interface resistance: $R_{if} * L = 0.01\, n\Omega\, m$.

The same model has been used to analyse the effect of welding only the margins of the contact surface. This feature was obtained setting only a part of the contact surface at zero potential (Fig. 3d).

Finally the model shown in Fig. 3e was used to analyse the effect of an Aluminum degradation ($RRR = 50$) in a region 2 mm thick on each side of the weld.

3.3 Numerical analysis results

Some examples of the distribution of the equipotential lines resulting from these analyses are shown in Figs. 3 and 4. The same number of equipotential surfaces were put in every plot. Some considerations can be done looking at these distributions:

- the value of the interface resistance changes the way in which the current flows from the insert to the matrix, therefore the effect of this resistance is more than simply additive to the resistance of the matrix alone,
- in case of welding the narrow side of the conductor the current density distribution is almost uniform where it crosses the weld, while it's not uniform in case of welding the broad side (for this reason it's necessary a new model to analyse the effect of an RRR degradation in case of welding the broad side, while in the other case the effect is only additive),
- when the welding depth is only 3 mm, there is only a slight difference between a weld on the broad side of the conductor or on the narrow one.

The resulting values of the Φ function (i.e. the total resistance of a 1 meter welding) for the three welding configurations are reported in Tables 1,2 and 3.

TABLE 1: Resistive function Φ depending on: the resistance of the stabilizer-matrix interface, the side of the conductor on which the weld is done, the welding depth: all the conductor surface or 3 mm only on both sides.

	1	0.1	0.01	0	$(n\Omega\ m)$	$\Phi\,(interface)$
	$\Phi\,(welded\ conductor)$					
narrow	2.42	0.46	0.24	0.18	$(n\Omega\ m)$	Full penetrating welding
side	2.48	0.52	0.30	0.24	$(n\Omega\ m)$	3+3 mm welding depth
broad	2.20	0.25	0.046	0.017	$(n\Omega\ m)$	Full penetrating welding
side	2.40	0.44	0.22	0.16	$(n\Omega\ m)$	3+3 mm welding depth

Results are shown for four values of the stabilizer-matrix interface resistance: 1, 0.1, 0.01 and 0 $n\Omega$ for a 1 meter sample. Two welding techniques have been compared: the first resulting in a full penetrating weld, the second welding only 3 mm at both sides of the contact surface. The effect of a degradation of the Al matrix around the welded area, resulting in an RRR value of 50, has also been studied (Table 2).

The effect of soldering the Rutherford cables has been studied only analytically, and is here reported for comparison. The study has been done using two different techniques. In both the cases the current is supposed to flow from one cable to the other only through the adjacent faces (the largest). In the first case the soldering has been supposed a uniform SnPb sheet 0.3 mm thick. In the second case the technique shown by Wilson[1] has been adopted using the "typical" value of 0.1 for the ratio between the minimum distance of adjacent strands and their diameters (the resulting value for the adjacent strands distance is 0.13 mm). The value obtained was divided by 16 that is half the strands number (i.e. the number of the strands on a face).

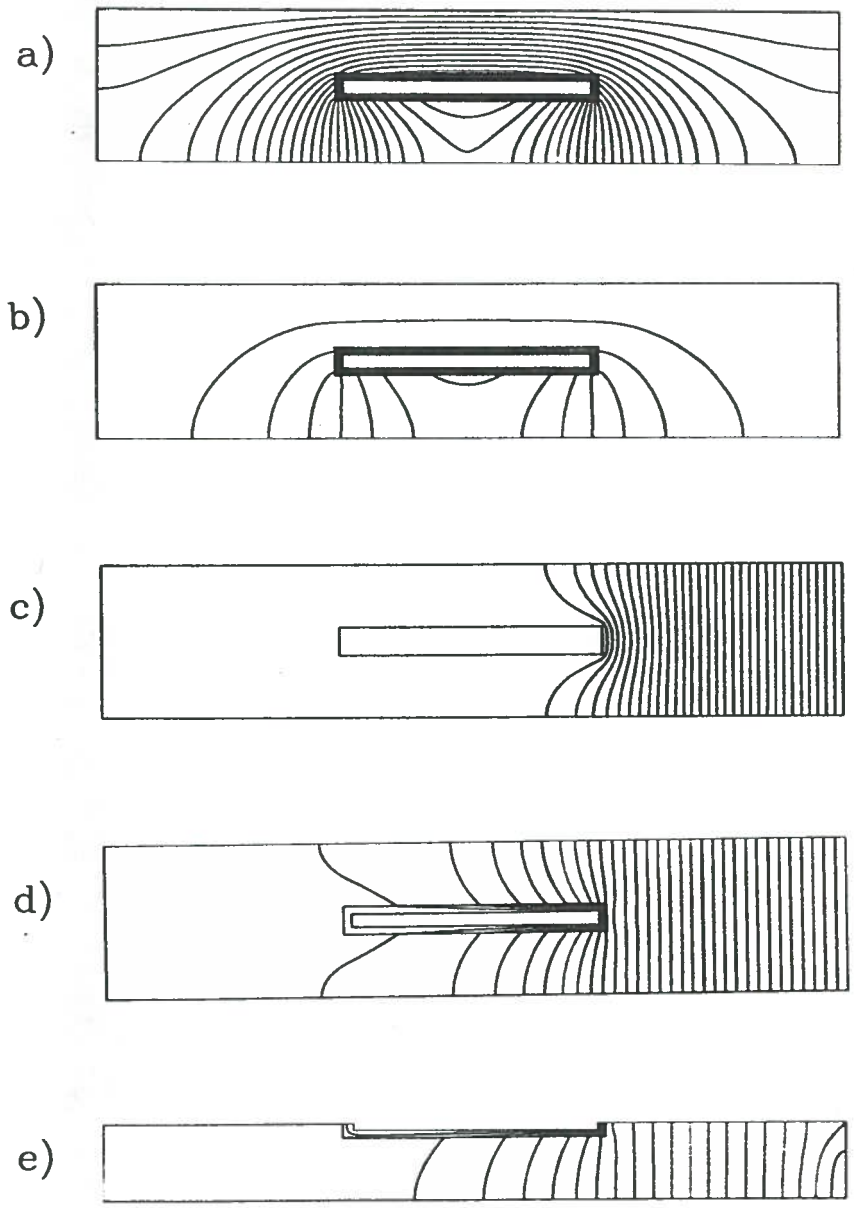

FIG. 4: Equipotential surfaces in case of welding the broad side: a) and b) interface resistance times lenght = 0.01 and 0.1 $n\Omega\, m$ respectively (see previous figure for more examples); in case of welding the narrow side: c) no interface resistance; d) interface resistance times lenght = 0.01 $n\Omega\, m$; e) welding depth 3 mm only.

3.4 Expected resistances in the Barrel Toroid junctions

The parameters for the analysis of the junctions in the ATLAS Barrel Toroid (and Bo coil) are summarized in the Table 4.

Fig. 5 shows the resistive function (Φ) (for a 3+3 mm welding depth) and the minimum lengths L_{min} of the three types of junction deduced by the more stringent condition (20).

In the Table 5 the expected resistive function (Φ_{exp}) the minimum and the suggested lengths (L_{min} and L_{sugg}) and the expected resistances ($R_{exp} = \Phi_{exp} \times L_{sugg}$) for the

TABLE 2: Resistive function Φ depending on the same parameters as above, adding a degradation of the Al matrix (RRR=50) in a region 4 mm thick around the weld.

	1	0.1	0.01	0	$(n\Omega\, m)$	$\Phi\,(interface)$
	$\Phi\,(welded\ conductor)$					
narrow	2.58	0.62	0.40	0.34	$(n\Omega\, m)$	Full penetrating welding
side	2.81	0.85	0.63	0.57	$(n\Omega\, m)$	3+3 mm welding depth
broad	2.24	0.29	0.082	0.054	$(n\Omega\, m)$	Full penetrating welding
side	2.75	0.79	0.57	0.49	$(n\Omega\, m)$	3+3 mm welding depth

TABLE 3: Resistance of a soldered junction between the inserts (Rutherford cables). Current is supposed to flow only through the adjacent cable faces. Results of a uniform soldering sheet approximation and of the technique used by Wilson are shown.

$3\,10^{-9}$	$3\,10^{-9}$	$(\Omega\, m)$	SnPb resistivity
0.3		(mm)	uniform sheet thickness
	0.1		minimun_distance/strand_diameter
0.045	0.038	$(n\Omega\, m)$	$\Phi\,(soldered\ inserts)$

three types of junction are summarized.

Each type of junction fulfils the condition (21) with a large margin so that in principle each of them can be used in the BT or Bo coil. The choice of the junction type will be determined by a compromise between thermal, electrical and mechanical requirements.

TABLE 4: Physical and geometrical parameters of the conductor and junction in the Barrel Toroid and Bo coil.

Parameter	Symbol	Value
Dimensions of the conductor		$57 \times 12\, mm^2$
Dimensions of the insert		$20 \times 2.3\, mm^2$
Cross section of the matrix	S	$6.3\,10^{-4}\, m^2$
Cooled perimeter of the conductor	p	$1.2\,10^{-2}\, m$
Thickness of the insulation	Δ	$1.5\,10^{-3}\, m$
Maximum current intensity	I	$20500\, A$
Thermal conductivity of the insulation	k_{is}	$1.0\, W/Km$
Thermal conductivity ratio	k_{is}/k	10^{-3}
Maximum temperature drop	$\theta_{max} - \theta_o$	$0.2\, K$
Thickness of the Cu-Al interface	t_{if}	$10^{-4}\, m$
Thickness of the welded region	t_w	$4\,10^{-3}\, m$
Resistivity of the interface	ρ_{if}	$5.0\,10^{-9}\, \Omega m$
Resistivity of the welded region	ρ_w	$5.0\,10^{-10}\, \Omega m$
Resistivity of the matrix	ρ	$6.0\,10^{-11}\, \Omega m$

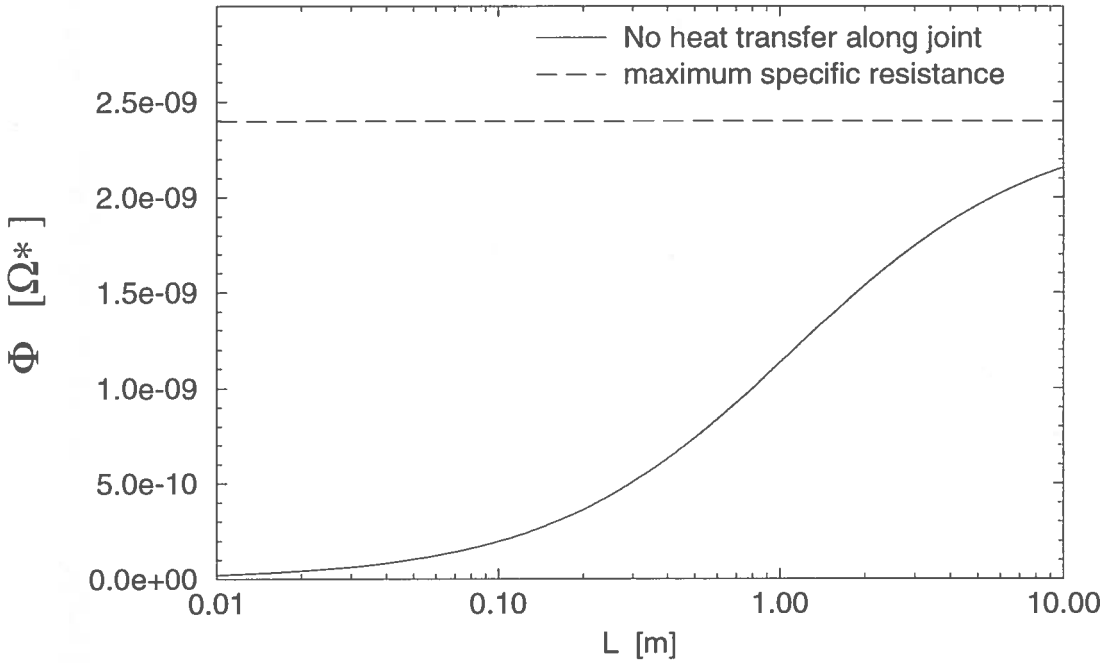

FIG. 5: Expected specific resistances and minimum lengths for the three types of junctions in the BT or Bo conductor .

TABLE 5: Expected parameters of the three types of junction. ($\Phi_\infty = 2.4\,10^{-9}\,\Omega$)

Parameter	Type I	Type II	Type III
$\Phi_{exp}\,(\Omega\,m)$	$8.5\,10^{-10}$	$7.9\,10^{-10}$	$\sim 5.0\,10^{-11}$
$L_{min}\,(m)$	0.62	0.55	0.024
$L_{sugg}\,(m)$	≥ 1.0	≥ 1.0	~ 0.2
$R_{exp}\,(\Omega)$	$\leq 8.5\,10^{-10}$	$\leq 7.9\,10^{-10}$	$\sim 2.5\,10^{-10}$

4 CONCLUSIONS

The first type of junction is the most probable candidate for the pancake connection inside the casing, the second one probably is the most suitable for the connection between double pancakes and between coils of the toroid, the third one is the only possible if a repair of the conductor is required.

For these reasons the LASA, with the firm charged of the Bo coil construction, will test all types of junction in order to verify the procedure, the experimental values of the junction resistances and the mechanical properties.

REFERENCES

(1) M. N. Wilson *"Superconducting Magnets"*, Clarendon Press Oxford (1983), p. 314.